Available online at www.sciencedirect.com
SCIENCE DIRECT
Journal of Photochemistry and Photobiology A: Chemistry 173 (2005) 128–136
Journal of Photochemistry and Photobiology A:Chemistry
www.elsevier.com/locate/jphotochem

Characterization of Bi/TiO_2 nanometer sized particle synthesized by solvothermal method and CH_3CHO decomposition in a plasma-photocatalytic system

Misook Kang [a,*], Yu-Ri Ko [b], Min-Kyu Jeon [b], Sung-Chul Lee [b], Suk-Jin Choung [b], Jong-Yul Park [c], Sung Kim [d], Suk-Ho Choi [d]

[a] *Industrial Liaison Research Institute, Kyung Hee University, Yongin, Gyeonggi 449-701, South Korea*
[b] *Department of Chemical Engineering, Kyung Hee University, Yongin, Gyeonggi 449-701, South Korea*
[c] *Department of Chemistry, Pusan National University, Jangjeundong 30, Kumjongku, Pusan 609-735, South Korea*
[d] *College of Electronics and Information and Institute of Natural Sciences, Kyung Hee University, Yongin, Gyeonggi 449-701, South Korea*

Received 6 May 2004; received in revised form 11 November 2004; accepted 29 December 2004
Available online 17 February 2005

Abstract

This study focuses on the relationship between the plasma-photocatalytic activity for CH_3CHO (acetaldehyde) decomposition and the surface properties of pure TiO_2 and 10.0 mol% Bi/TiO_2 nano-sized. The TiO_2 and Bi/TiO_2 particles, which were synthesized through the solvothermal method, exhibited a uniformly spherical anatase structure with particle size below 25 nm. The surface area was large (310 m^2/g) as compared with that of pure TiO_2 (140 m^2/g). Bi/TiO_2 adsorbed a smaller amount of water than pure TiO_2. From the H_2-TPR result, it was identified that Ti^{3+} could be easily transferred into Ti^0, which affected the photoreaction, over Bi/TiO_2 compared with pure TiO_2. Based on these results, without H_2O addition, acetaldehyde decomposition was higher on Bi/TiO_2 (80% after 40 min). In particular, the by-product (mainly CH_3COOH), a serious problem in the plasma system, was very small in Bi/TiO_2 (below 5.0%) compared with that in pure TiO_2, which was above 20.0%. However, the acetaldehyde removal slightly increased over Bi/TiO_2 with H_2O addition, while it remarkably enhanced over pure TiO_2. This result means that H_2O addition did not have a good influence on acetaldehyde removal over the Bi/TiO_2 with hydrophobic property. However, it did exert a better influence on pure TiO_2 with hydrophilic property.

Keywords: Bi/TiO_2; H_2-TPR; CH_3CHO decomposition; H_2O addition; Plasma-photocatalytic system

1. Introduction

The world faces a tremendous set of environmental problems. Thus extensive research activities are carried out in search of advanced chemical, biochemical, and physicochemical methods to eliminate hazardous chemical compounds from air and water [1–3]. Many studies have been done on the photocatalytic treatment of environmental pollutants using semiconductors like TiO_2, Fe/TiO_2, and Zn/TiO_2. To develop a more effective and low-cost method for VOC decomposition, further extensive research using TiO_2 photocatalytic system was performed. However, this system has not resulted in giving better photoactivity for application in industrial division [4–6].

Several papers have reported that these problems could be overcome by using discharge plasma as a driving light source of photocatalysis [5–7]. Strong plasma is expected to promote the excited rate of the electron on the surface of TiO_2 catalyst compared with UV-irradiation (Fig. 1). The figure confirms that plasma was emitted and it was similar with that of UV-lamp. It corresponds to 3–4 eV. It was thought that photocatalysis could be possible using plasma as a light source. Consequently, the VOC decomposition should be increased. To date, however, the system also has some problems. In particular, an important issue regarding the use of the plasma

* Corresponding author. Tel.: +82 31 201 2121; fax: +82 31 202 4765.
E-mail address: mskang@khu.ac.kr (M. Kang).

1010-6030/$ – see front matter © 2005 Elsevier B.V. All rights reserved.
doi:10.1016/j.jphotochem.2004.12.030

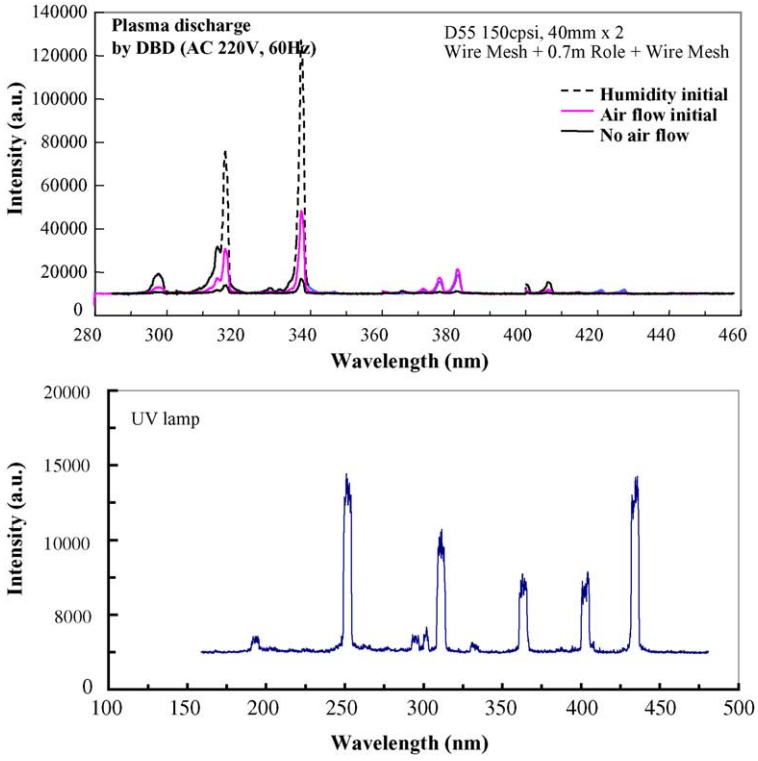

Fig. 1. Emission spectra analysis of discharge plasma and UV-lamp of 365 nm.

process for removing VOC is the treatment of inorganic and organic by-products emitted from the process.

The main objective of this study is to enhance gas-phase acetaldehyde decomposition activity using dielectric barrier discharge (DBD) plasma. The acetaldehyde is a main malodorous VOC extracted from industrial processing. This is operated at atmospheric condition as a photocatalytic light source to suppress the formation of secondary products. A previous research attempted to solve the introduction of Al/TiO_2 including Al_2O_3 having higher hydrophilic property to benzene plasma-photocatalytic decomposition [8]. The result shows that the plasma-photocatalytic system shows a high possibility for VOC (especially aromatic macro molecules) decomposition.

Therefore, in this study, the plasma-photocatalytic system was applied with and without H_2O addition to decompose acetaldehyde over 10.0 mol% Bi/TiO_2 nanometer sized photocatalyst. In addition, the surface properties of Bi/TiO_2 were characterized in detail.

2. Experimental

2.1. Catalyst preparation

This study considered a commonly solvothermal method [9] to synthesize Bi/TiO_2 nanometer particles as shown in Fig. 2. The reagents used for the preparation of sol-mixture were titanium tetra-isopropoxide or TTIP (99.95%, Junsei Chemical, Japan) and bismuth (III) chloride (99.99%, Junsei Chemical, Japan), which were used as Ti and Bi precursors. Metal precursors were mixed with ethyl alcohol (99%, Wako Pure Chem. Ltd.) in an autoclave (model R-211, Reaction Engineering Inc., Korea) heated at 200 °C for 10 h at a rate of 10 °C/min. The molar ratios of Bi:Ti precursors in gel mixtures were kept to molar ratio of 1:10. During thermal treatment, Ti and Bi were hydrolyzed by the OH group in solvent and then the crystallized nano-sized Bi/TiO_2 occurred. The resulting powder was washed with distilled water until pH 7 and then dried. Finally, to remove impurities, which remained carbon or chloride ions on surface of the powders, these samples were thermal treated at 500 °C for 3 h.

2.2. Characterizations of synthesized catalyst

The synthesized samples, Bi/TiO_2 nanometer powders, were identified by powder X-ray diffraction analysis (XRD, model PW 1830 from Philips) with nickel filtered Cu Kα radiation (30 kV, 30 mA) at 2θ angles from 5° to 70°. The scan speed was 10°/min and the time constant was 1 s. The particle size and shape of the powders were observed through scanning electron microscopy (SEM and FESEM, model JEOL-JSM35CF). The power was set at 15 kV. The UV–visible spectrum was obtained using a Shimadzu MPS-2000 spectrometer with a reflectance sphere. The spectral range was from 200 to 700 nm. The BET surface area of the sample and pore size distribution (PSD) were measured through nitrogen gas adsorption in a continuous flow method using a chromatograph equipped with a TCD detector at the liquid nitrogen temperature. A mixture of nitrogen and helium was

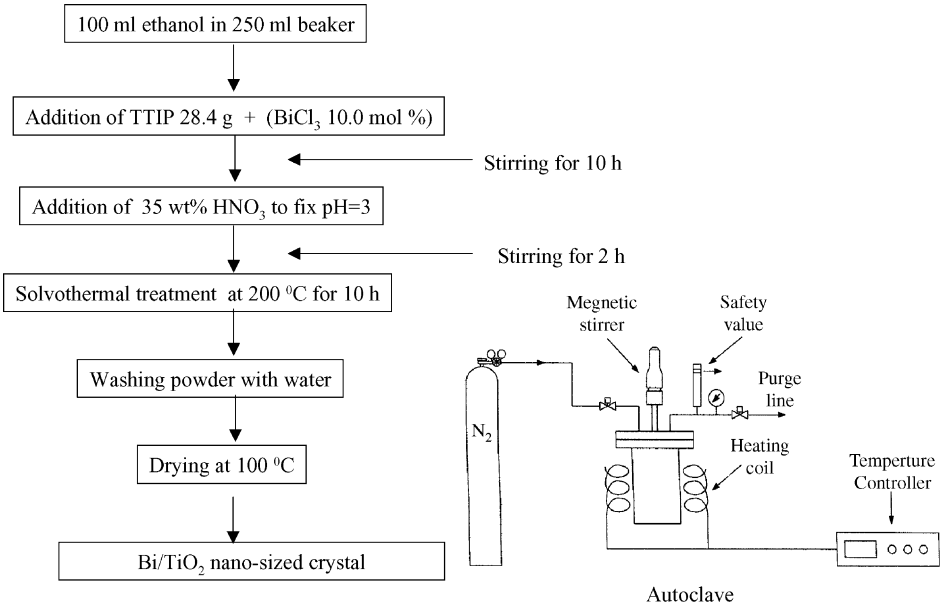

Fig. 2. Preparation of TiO_2 and 10.0 mol% Bi/TiO_2 nanometer particles by solvothermal method.

flowed as the carrier gas with the GEMINI2375 model from Micrometrics. The sample was thermally treated at 350 °C for 3 h before nitrogen adsorption. To analyze the binding energy between Ti 2p and O 1s, X-ray photoelectron spectroscopy (XPS, PHI 5700, PHI com.) was employed. Fresh catalysts were prepared with 1.0 mm pellets and then treated in vacuum overnight prior to measurement. The Al mono (pass energy = 23.5 eV) was used as X-ray source at 350 W power, 15 kV, and pressure of below 2.7×10^{-6} Pa during the measurement. In Raman spectroscopy, a laser is directed at the sample. The majority of the light is inelastically scattered (Rayleigh light). However, a small fraction is scattered elastically. The energy difference between the incident and reflected beam often measured in wave number (cm^{-1}) corresponds to a change in molecular vibration within the sample. Therefore, characteristic bond vibrations allow the chemical and crystal state identification of the sample. Raman spectra were acquired on RFS 100/s FT-Raman spectrometry. The wave number values reported from the spectra were accurate within 4.0 cm^{-1}. The emission line at 1064 nm from Ld-YAG laser (spectra physics) was focused on the sample under a microscope, and the analyzed spot was ~1 μm. The power of the incidents beam on the sample was 102 mV. The photoluminescence (PL) spectroscopy measurement was also tested to examine the number of photo-excited electron–hole pairs for all samples. Samples of 1.0 mm pellet type were measured at liquid nitrogen temperature (room temperature and 8 K) using He–Cd laser source of 325 nm.

2.3. Adsorption and desorption of H_2, H_2O, and NH_3

NH_3-temperature programmed desorption (TPD) measurements were carried out on a conventional TPD system equipped with a TCD cell. The catalysts were exposed to He gas at 550 °C for 2 h in order to remove water and impurities on surface. After pretreatment, the samples were exposed to ammonia for 1 h. Finally, the programmed heating at a rate of 10 °C/min was started and then followed by heating to 700 °C. The amount of desorbed gas was continuously monitored with a TCD cell.

H_2-TPR (temperature programmed reduction) followed. About 0.3 g of catalysts was pretreated under He flow (30 mL/min) at 550 °C for 2 h, and then cooled to room temperature. Analysis was carried out by flowing 30 mL/min of H_2 (10 vol.%)/N_2 and raising the catalysts' temperature from room temperature to 550 °C at 5 °C/min. The change in hydrogen concentration was measured using gas chromatograph (GC series 580, GOW-MAC) equipped with a TCD.

The dehydration and activation energies for H_2O decomposition in catalysts were determined using a TG–DSC equipped with a micro-thermo-differential and gravimetric analyzer (Perkin Elmer Co., USA). A weight of 20 mg α-alumina was used as reference sample. To keep the moisture conditions identical, the sample was analyzed after contact with saturated NH_3Cl solution for 24 h.

2.4. Analysis of product for decomposition of acetaldehyde in plasma-photocatalytic system

As shown in Fig. 3, the plasma-photocatalytic reactor consists of an emitting stainless steel rod held in the center of the reactor, a wrapping thin wire sheet, and small-sized beads. The reactor made from quartz glass was fixed with a diameter of 25 mm and length of 240 mm. AC high-voltage was supplied with an amplifier (KSA-15/05CA) and a function generator (EZ digital, FG-7002C). The waveform of the pulse voltage and current were measured using a digital oscilloscope with the voltage divider and current probe. The input

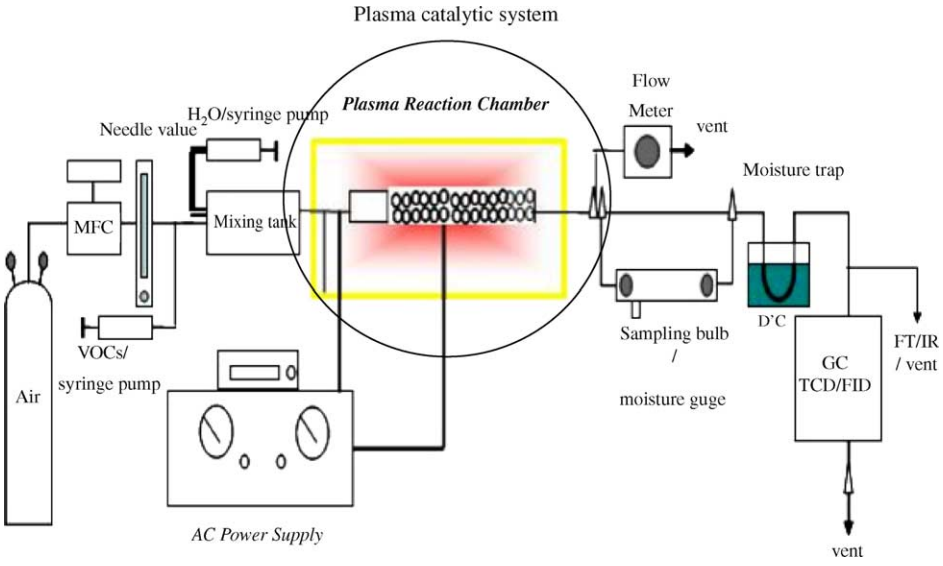

Fig. 3. Schematic representation of discharge plasma reactor apparatus.

power was measured using a digital power meter at the wall plug of the transformer. This value included the discharge power as well as energy loss in the power source. Generated radiation powers were attained through the regulation of the current and pulse voltage. The *V–Q* method was used to determine the discharge power in the plasma reactors. The charge *Q* was determined by measuring the voltage across the capacitor of 1 μF connected in series to the ground line of the plasma reactors [10]. The energy transferred from the power source to the plasma reactor was 20–30%. The intensities of pulse voltages were 7.0 kV and the frequency of currents was 600 Hz. The discharge power was calculated from the area of *V–Q* parallelogram by multiplying the frequency. Specific input energy (SIE) was calculated with the following relations:

$$\text{Specific input energy (J/L)} = \frac{\text{discharge power (W)}}{\text{gas flow rate (L/min)}}$$

SIE value was varied by changing either the applied voltage or the frequency [11].

The 10.0 mol% Bi/TiO_2 particles were fixed on glass beads using a silane binder. The acetaldehyde concentration was fixed to 100 ppm. During the plasma-photocatalytic degradation, 10 mol% H_2O was added to confirm the influence of the OH group. On the other hand, to determine the catalytic lifetime, the acetaldehyde removal was carried out in a continuous system with a carrier gas at the flow rate of 300 mL/min of O_2 gas.

The products in plasma-photocatalytic decomposition were analyzed by a TCD-type gas chromatograph (GC). The conditions of GC were as follows—detector: TCD, column: Chromosorb 102, injection temperature: 200 °C, initial temperature: 40 °C, final temperature: 200 °C, detector temperature: 200 °C.

3. Results and discussion

3.1. Characterization

Fig. 4 shows the X-ray diffraction (XRD) patterns of TiO_2 and 10.0 mol% Bi/TiO_2 powders of as-synthesized and after thermal treatment at 500 °C for 3 h. In general, the TiO_2 pho-

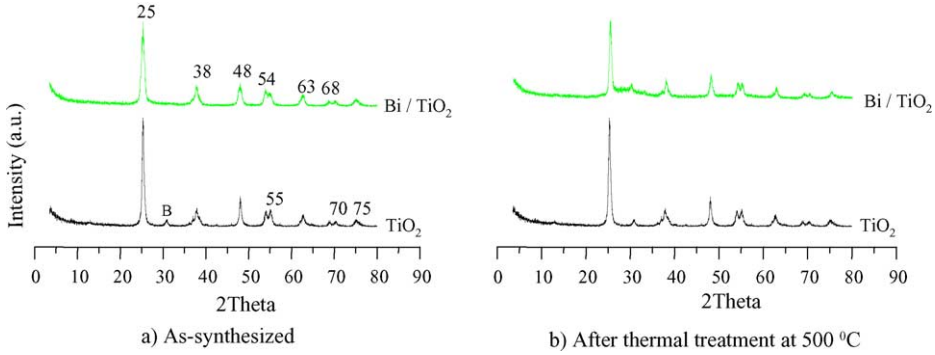

Fig. 4. XRD patterns of TiO_2 and 10.0 mol% Bi/TiO_2 nanometer particles prepared by solvothermal method: (a) as-synthesized; (b) after 500 °C.

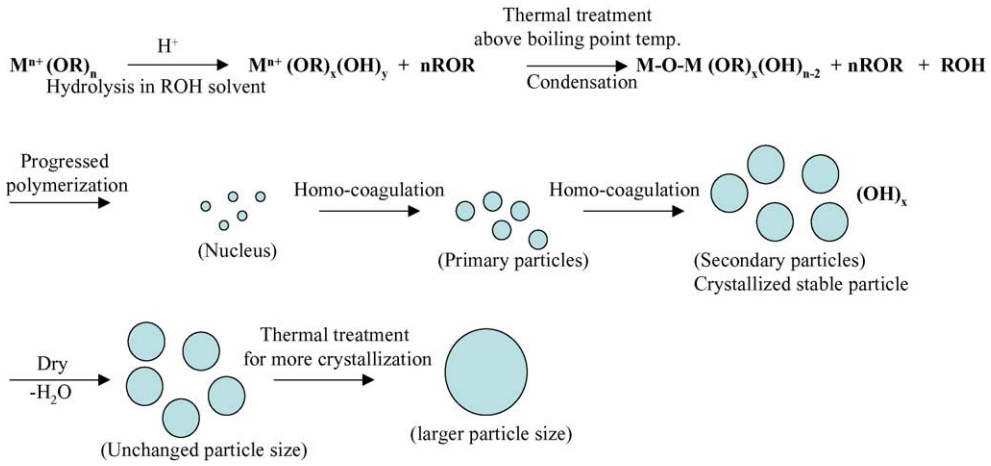

Scheme 1. The expected mechanism of metal oxide nanometer particle by solvothermal method.

tocatalyst with anatase structure was attained in the sol–gel process after calcination step at 500 °C for 3 h. However, it could acquire just as-synthesized in solvothermal method without any other treatment. The reason is illustrated in Scheme 1: unlike in the sol–gel method, the crystallized TiO_2 nucleus occurred in thermal treatment in high temperature and pressure, and then grew up to primary particle through homo-coagulation. At this point, the excess solvents partially suppressed more crystal growth; as a result, the particle size became finer than that in the sol–gel method. Finally, the TiO_2 anatase particles were attained without the calcination step. On the other hand, the anatase structure exhibited higher performance for VOC decomposition compared with catalysts of other structures, like rutile, brookite, and amorphous.

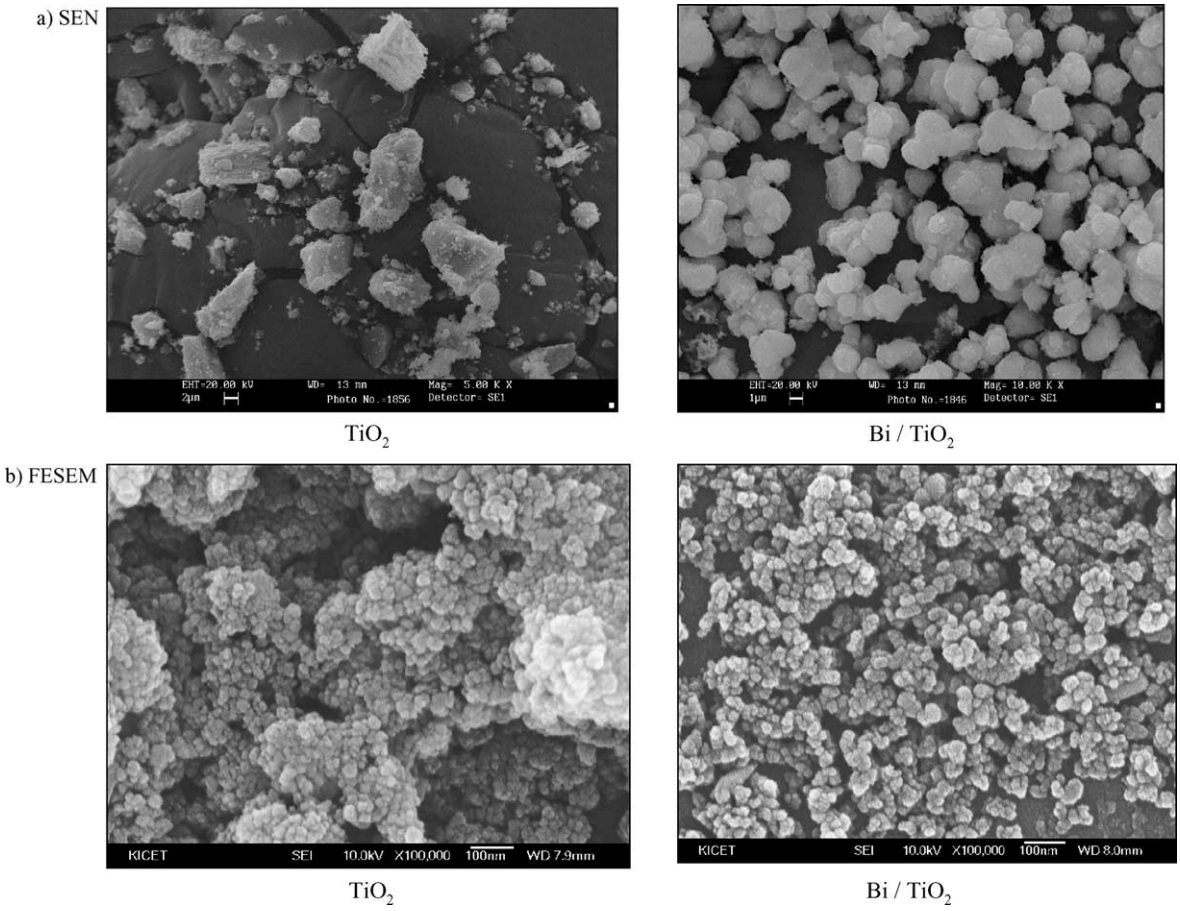

Fig. 5. SEM and FESEM photographs of TiO_2 and 10.0 mol% Bi/TiO_2 nanometer particles prepared by solvothermal method: (a) SEM image; (b) FESEM image.

The samples, TiO_2 and Bi/TiO_2, showed a well-developed anatase structure, the same as that after 500 °C. This result means that the Bi ion was well inserted into the Ti site in anatase structure. The peak width was slightly broader for Bi/TiO_2 compared with that of pure TiO_2 particle. In general, the width of XRD peak corresponded to the crystallite sizes of materials. When the width was broad, the crystallites had smaller sizes. Therefore, from this figure, it was suspected that Bi/TiO_2 particles were smaller and thermally more stable than pure TiO_2 particles.

Fig. 5 shows the SEM and FESEM photographs of particle shape and size distribution of TiO_2 and Bi/TiO_2 catalysts. Two catalysts were shown to consist of relatively uniform and spherical particles with sizes of about 25 nm in FESEM. The multi-particles were regularly distributed by coagulation in the case of the 10.0 mol% Bi/TiO_2 while the particles were irregularly distributed in pure TiO_2. This result could be attributed to the charge effect on the catalysts' surface.

Raman spectroscopy has been extensively used to study TiO_2. It was worthwhile to include this technique since it is a rapid way of obtaining the surface crystal structure of TiO_2. Fig. 6 shows the Raman spectra of TiO_2 and 10.0 mol% Bi/TiO_2. These spectra could be ascribed to the anatase phase. Ohsaka et al. recorded the reference Raman spectra of the powders of anatase (bonds at 639, 519, 513, 399, 197, and 144 cm^{-1}) [12,13]. The primitive unit cell contains two TiO_2 formula units. Factor group analysis indicates the existence of six optical modes with the following irreducible representation of normal vibrations: $1A_{1g} + A_{2u} + 2B_{1g} + 1B_{2u} + 3E_g + 3E_u$. The modes of A_{1g}, B_{1g}, and E_g are Raman active and those of A_{2u} and E_u are infrared active. In this figure, the peaks of TiO_2 and Bi/TiO_2

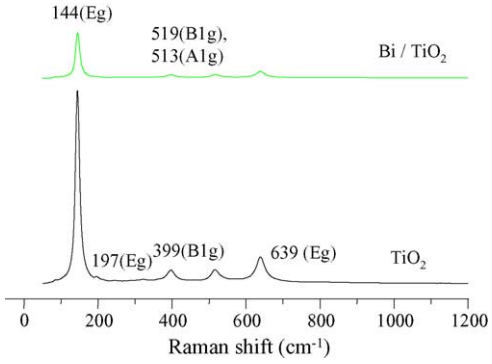

Fig. 6. Raman spectroscopy of TiO_2 and 10.0 mol% Bi/TiO_2 nanometer particles prepared by solvothermal method.

were the same, although a decrease in peak intensity was observed in Bi/TiO_2. The results of XRD and Raman spectroscopy confirm that the Bi ions were well substituted to Ti sites.

Table 1 summarizes the physical properties of the TiO_2 and Bi/TiO_2 catalysts. The Bi/TiO_2 real composition attained by ICP was accorded to the amount of precursor added in sol preparation. The table also gives the pore volume and pore diameter. When Bi was added into titanium dioxide, the new bulk pore of about 46 Å was generated. From this result, the BET surface area also increased, reaching to about 310 m^2/g in 10.0 mol% Bi additions. However, it was confirmed that the surface area increased in TiO_2 (140 m^2/g) synthesized by solvothermal method.

Quantitative XPS analysis was performed on the TiO_2 and 10.0 mol% Bi/TiO_2 particles [14,15]. Typical survey and high-resolution spectra are presented in Fig. 7(a). The survey

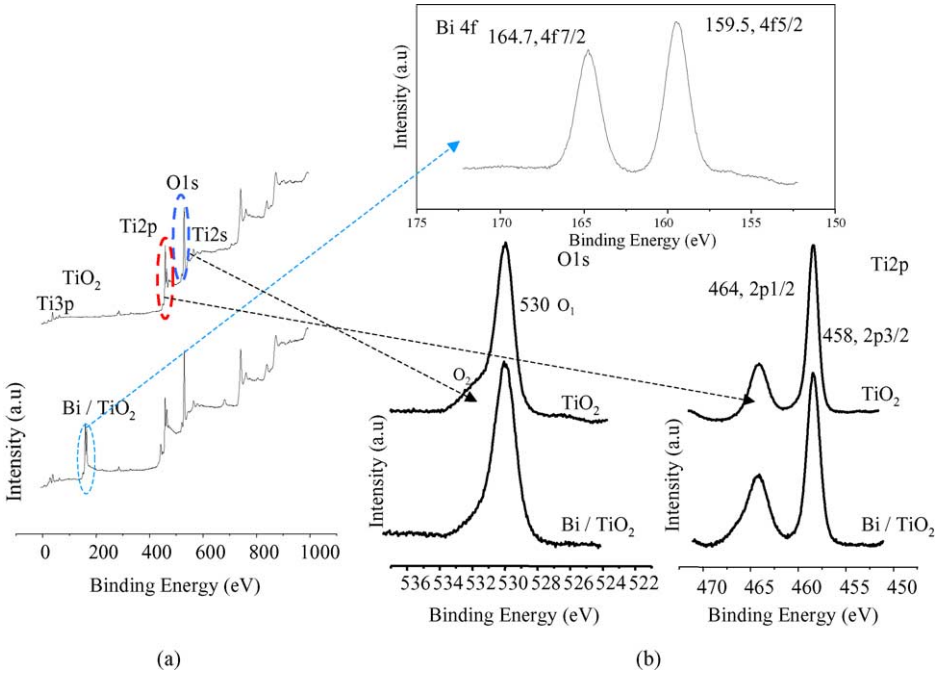

Fig. 7. XPS spectroscopy of TiO_2 and 10.0 mol% Bi/TiO_2 nanometer particles prepared by solvothermal method: (a) full range; (b) partial range.

Table 1
Physical properties of synthesized nano-sized Bi/TiO_2 powder

Catalysts	Composition on surface (at.%)			Average pore size (Å)	Average pore volume (mL/g)	Surface area (m^2/g)
	Bi	Ti	O			
TiO_2	–	25.0	75.00	–	–	140
Bi/TiO_2	2.37	23.62	74.02	46	1.56	310

spectra of the TiO_2 and 10.0 mol% Bi/TiO_2 particles contained the Ti 2p and O 1s peaks from TiO_2. The Ti $2p_{1/2}$ and Ti $2p_{3/2}$ spin–orbital splitting photoelectrons for both samples were located at the binding energies 464 and 458 eV, respectively. In general, large binding energy means more oxidized metal. However, in both catalysts, the intensity and shift of these curves were not changed. On the other hand, the Gaussian values were used in the curve resolution of the individual O 1s peaks (first peak O1: 530 eV, second peak O2: 532 eV) in the two spectra. The curve-resolved O 1s signed of the TiO_2 and 10.0 mol% Bi/TiO_2 particles resulted in a second peak located at a binding energy of 532 eV. This secondary peak was assigned to OH species, bulk oxide (O^{2-}), or H_2O adsorption on the surface [15]. This was not shown in the Bi/TiO_2 framework. The results indicate that Bi/TiO_2 has hydrophobic property.

To confirm the effect of Bi addition into titanium dioxide framework, the NH_3-TPD test was performed. Fig. 8 shows the resulting profiles. Generally, these profiles consist of two peaks: one appearing at a low temperature range around 200–300 °C and the other appearing at a high temperature range around 450–550 °C. The low and high temperature peaks correspond to the weak and strong acid sites, respectively. However, in the case of pure TiO_2, only the one peak assigned to NH_3 physical desorption was found around 100 °C, while the two peaks for NH_3 adsorption around 100 and 200 °C were shown in 10.0 mol% Bi/TiO_2 sample. This result explains that the new acid sites on TiO_2

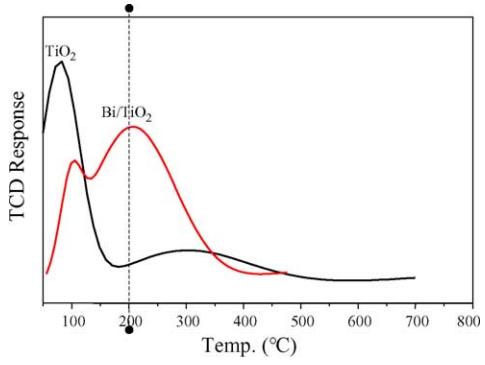

Fig. 8. NH_3-TPD profiles of TiO_2 and 10.0 mol% Bi/TiO_2 nanometer particles prepared by solvothermal method.

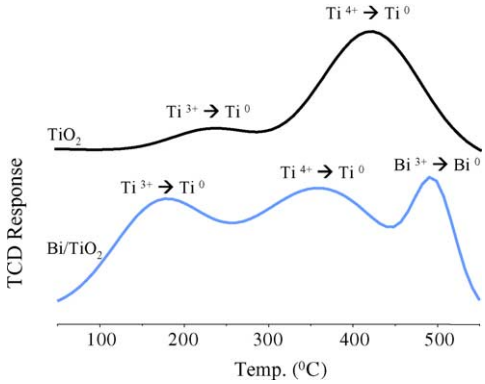

Fig. 9. H_2-TPR curves of TiO_2 and 10.0 mol% Bi/TiO_2 nanometer particles prepared by solvothermal method.

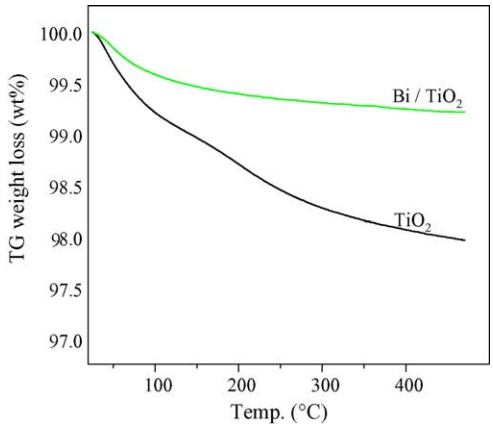

Fig. 10. TG curves of TiO_2 and 10.0 mol% Bi/TiO_2 nanometer particles prepared by solvothermal method.

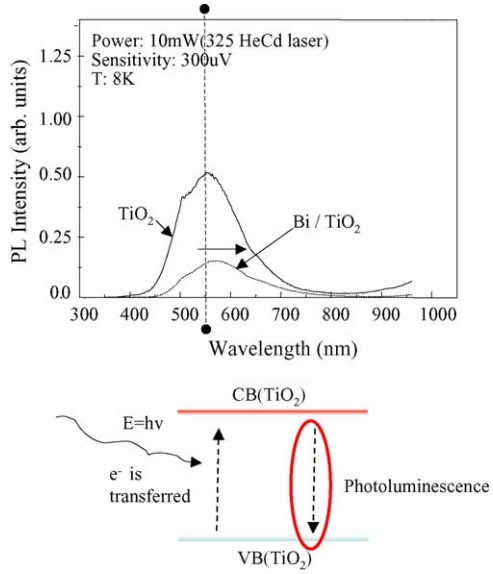

Fig. 11. PL curves of TiO_2 and 10.0 mol% Bi/TiO_2 nanometer particles prepared by solvothermal method.

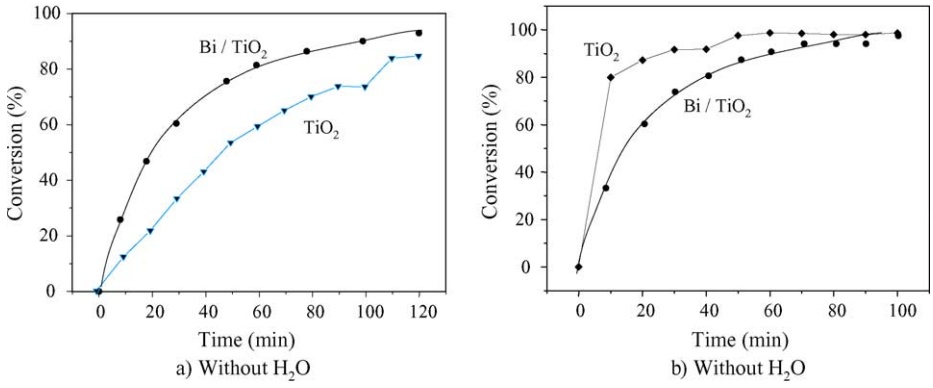

Fig. 12. Acetaldehyde decomposition with and without 10.0 wt.% H_2O addition over TiO_2 and 10.0 mol% Bi/TiO_2 nanometer particles in plasma-photocatalytic system. Reaction conditions: acetaldehyde concentration, 100 ppm; catalyst weight, 1.5 g; plasma intensity, 9.0 kV, 0.5 mA, 1.0 kHz, 0.45 kW; batch system.

photo-catalyst framework were generated by addition of Bi. Therefore, these acid sites could partially attract acetaldehyde molecules.

Generally, photocatalysis is an oxidation–reduction reaction by electron and hole. H_2-TPR experiments have been applied for investigation into the reduction behavior of catalysts. Fig. 9 gives the reduction profiles of TiO_2 and 10.0 mol% Bi/TiO_2. It has been suggested that Ti^{3+} is first reduced to Ti^0 at the lower temperature, while the higher temperature peak corresponds to the reduction of Ti^{4+} to Ti^0. In general, the photoreaction was related to the reduction of Ti^{3+} into Ti^0. According to the TPR profile, upon addition of Bi, the reduction of Ti^{3+} into Ti^0 easily occurred. Therefore, it could be suggested that 10.0 mol% Bi/TiO_2 catalyst has a higher photoactivity than pure TiO_2.

Fig. 10 compares the amount of water desorbed in the photocatalysts calculated from TG curve. With addition of Bi in photocatalyst, the amount of water adsorbed also decreased. This result could be attributed to the more hydrophobic property of the 10.0 mol% Bi/TiO_2 (0.5 wt.% H_2O loss) than pure TiO_2 (2.0 wt.% H_2O loss). Generally, the hydrophilic property of the photocatalyst has a better effect in photoactivity.

Fig. 11 shows the photoluminescence spectroscopy of TiO_2 and Bi/TiO_2 photocatalysts. The PL curve means that the electron in valence band transferred more easily to the conduction band, and then the excited electrons were stabilized with photoemission. Therefore, if the PL intensity was increased in the same wavelength, the photoactivity was also increased. However, this figure shows that the PL curve shifted to the right (the longer wavelength) in Bi/TiO_2 compared to pure TiO_2. This result means that the band gap of TiO_2 anatase was changed to low energy upon addition of Bi^{3+}.

3.2. CH_3CHO decomposition in plasma-photocatalytic system

Fig. 12 gives the CH_3CHO conversions with and without H_2O addition over TiO_2 and 10.0 mol% Bi/TiO_2 in batch plasma reactor system. According to a previous paper, the optimum H_2O amount was 10.0 wt.% per reactant [8]. In this study, 10.0 wt.% H_2O was also kept. Without H_2O addition, acetaldehyde decomposition was highest on Bi/TiO_2 (80% after 40 min). The by-product (mainly CH_3COOH), which is a serious problem in plasma system, was very small in Bi/TiO_2 (below 5.0%) compared with that in pure TiO_2, which was above 20.0%. The acetaldehyde removal slightly increased over Bi/TiO_2 with H_2O addition, while it remarkably enhanced over pure TiO_2. This indicates that H_2O addition did not have a good influence on acetaldehyde removal over the Bi/TiO_2 with hydrophobic property. However, it did exert a better influence on pure TiO_2 with hydrophilic property.

4. Conclusion

This study focuses on the relationship between the plasma-photocatalytic activity for CH_3CHO (acetaldehyde) and the surface properties of pure TiO_2 and 10.0 mol% Bi/TiO_2 nanometer sized. The main results are summarized in the following:

1. The TiO_2 and 10.0 mol% Bi/TiO_2 particles, which were synthesized through the solvothermal method, exhibited a uniformly spherical anatase structure with particle size below 25 nm.
2. The surface area was large (310 m^2/g) as compared with that of pure TiO_2 (140 m^2/g). Bi/TiO_2 (10.0 mol%) adsorbed smaller water amount than pure TiO_2.
3. The results of XRD and Raman spectroscopy showed that the Bi ions were well substituted to Ti sites.
4. TG curves and XPS results showed that the 10.0 mol% Bi/TiO_2 has hydrophobic property. The Ti^{3+} could be easily transferred into Ti^0 over 10.0 mol% Bi/TiO_2 compared with pure TiO_2.
5. In the case of pure TiO_2, only the one peak assigned to H_2O physical desorption was found around 100 °C, while the two peaks for NH_3 adsorption around 100 and 200 °C were shown in 10.0 mol% Bi/TiO_2 sample.

6. Without H_2O addition, acetaldehyde decomposition was higher on Bi/TiO_2 (80% after 40 min). In particular, the by-product (mainly CH_3COOH), a serious problem in plasma system, was very small in 10.0 mol% Bi/TiO_2 (below 5.0%), compared to the 20.0% by-products in pure TiO_2.
7. The acetaldehyde removal slightly increased over 10.0 mol% Bi/TiO_2 with H_2O addition, while it was remarkably enhanced over pure TiO_2.

Acknowledgement

This work was supported by Korea Research Foundation (KRF-2003-D00014). The authors are grateful for financial support.

References

[1] U. Stafford, K.A. Gray, P.V. Kamat, J. Catal. 167 (1997) 25.
[2] J.M. Hermann, Catal. Today 53 (1999) 115.
[3] S. Yamazaki, S. Tanaka, H. Tsukamoto, J. Photochem. Photobiol. A: Chem. 121 (1999) 55.
[4] G. Dagan, S. Sampath, Chem. Mater. 7 (1995) 446.
[5] J. Arno, J.W. Bevan, M. Moisan, Environ. Sci. Technol. 30 (1996) 2427.
[6] A. Dono, C. Paradisi, G. Scorrano, Rapid Commun. Mass Spectrosc. 11 (1997) 1687.
[7] M. Kang, B.-J. Kim, S.M. Cho, C.-H. Chung, B.-W. Kim, G.Y. Han, K.J. Yoon, J. Mol. Catal. A: Chem. 180 (2002) 125.
[8] B.-Y. Lee, S.-H. Park, M. Kang, S.-C. Lee, S.-J. Choung, Appl. Catal. A: Gen. 253 (2003) 371.
[9] M. Kang, S.-Y. Lee, C.-H. Chung, S.M. Cho, G.Y. Han, B.-W. Kim, K.J. Yoon, J. Photochem. Photobiol. A: Chem. 144 (2001) 185.
[10] Y.S. Mok, C.M. Nam, M.H. Cho, I.-S. Nam, IEEE Trans. Plasma Sci. 30 (2002) 408.
[11] H.-H. Kim, Y.-H. Lee, A. Ogata, S. Futamura, Catal. Commun. 4 (2003) 347.
[12] T. Ohsaka, F. Izumi, Y. Fujiki, J. Raman Spectrosc. 7 (1978) 321.
[13] P.S. Dobal, R.S. Katiyar, Y. Jiang, R. Guo, A.S. Bhalla, Int. J. Inorg. Mater. 3 (2001) 135.
[14] J.S. Dalton, P.A. Janes, N.G. Jones, Environ. Pollut. 120 (2002) 415.
[15] Y.-D. Wang, C.-L. Ma, X.-D. Sun, H.-D. Li, Appl. Catal. A: Gen. 8522 (1) (2003).